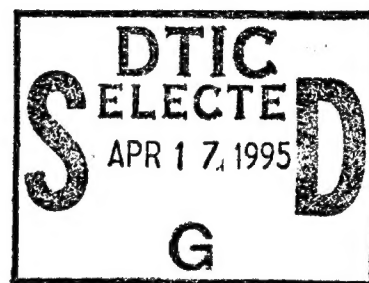# Naval Research Laboratory

Washington, DC 20375-5320

X-Band Magnicon Amplifier Research at the Naval Research Laboratory

STEVEN H. GOLD
ARNE W. FLIFLET

Beam Physics Branch
Plasma Physics Division

BAHMAN HAFIZI

Icarus Research
Bethesda, MD

DTIC
SELECTED
APR 1 7, 1995
G

April 19, 1995

19950414 127

REPORT DOCUMENTATION PAGE

1. AGENCY USE ONLY (Leave Blank)	2. REPORT DATE April 19, 1995	3. REPORT TYPE AND DATES COVERED Interim Report	

4. TITLE AND SUBTITLE

X-Band Magnicon Amplifier Research at the Naval Research Laboratory

5. FUNDING NUMBERS

6. AUTHOR(S)

Steven H. Gold, Bahman Hafizi,* and Arne W. Fliflet

7. PERFORMING ORGANIZATION NAME(S) AND ADDRESS(ES)

Naval Research Laboratory
Washington, DC 20375-5320

8. PERFORMING ORGANIZATION REPORT NUMBER

NRL/MR/6793--95-7666

9. SPONSORING/MONITORING AGENCY NAME(S) AND ADDRESS(ES)

Department of Energy
Washington, DC 20545

Office of Naval Research
Arlington, VA 22217

10. SPONSORING/MONITORING AGENCY REPORT NUMBER

11. SUPPLEMENTARY NOTES

*Icarus Research, Bethesda, MD 20814
Submitted to the Proceedings of the 1994 Workshop on Pulsed RF Sources for Linear Colliders, 3-10 October 1994, Montauk, NY.

12a. DISTRIBUTION/AVAILABILITY STATEMENT

Approved for public release; distribution unlimited.

12b. DISTRIBUTION CODE

13. ABSTRACT (Maximum 200 words)

We present a progress report on a program to develop a high-power second harmonic magnicon amplifier at 11.4 GHz for linear accelerator applications. The experiments are being carried out on the NRL Long-Pulse Accelerator Facility using a plasma cathode to create the electron beam. Typical beam parameters are 500 kV, 200 A, 5.5 mm diameter, with a ~300 nsec voltage flattop and a $~10^{-2}$ Hz repetition rate. An initial deflection cavity experiment demonstrated two-cavity gain of ~15 dB at a frequency ship of −0.18%, in good agreement with theory and simulation. A complete five cavity magnicon circuit was designed via computer simulation, fabricated, and cold tested. This circuit is now undergoing experimental tests. In preliminary experiments, a low power saturation effect was observed in the deflection cavities, apparently due to plasma formation caused by the diode x-ray flux and by inadequate vacuum conditions. Following a major effort to improve the vacuum and surface conditions, very recent experiments have shown that is possible to "burn through" this low power saturation effect, and achieve high fields in the deflection cavities. However, high power emission from the output cavity has not yet been observed. We are also evaluating new fourth magnicon designs via time-dependent multimode simulations.

14. SUBJECT TERMS

Magnicon	X-Band	Saturation
Amplifier	Gain	

15. NUMBER OF PAGES

10

16. PRICE CODE

17. SECURITY CLASSIFICATION OF REPORT	18. SECURITY CLASSIFICATION OF THIS PAGE	19. SECURITY CLASSIFICATION OF ABSTRACT	20. LIMITATION OF ABSTRACT
UNCLASSIFIED	UNCLASSIFIED	UNCLASSIFIED	UL

X–Band Magnicon Amplifier Research at the Naval Research Laboratory

Steven H. Gold,* Bahman Hafizi,† and Arne W. Fliflet*

*Beam Physics Branch, Plasma Physics Division,
Naval Research Laboratory, Washington, DC 20375
†Icarus Research, Bethesda, MD 20814

INTRODUCTION

The magnicon (1–4) is a scanning–beam microwave amplifier that is under consideration as a possible alternative to klystrons in powering future high–gradient linear electron accelerators. Scanning beam amplifiers modulate the insertion point of the electron beam into the output cavity in synchronism with the phase of a rotating rf wave. This synchronism creates the potential for an extremely efficient interaction in the output cavity, since every electron will in principle experience identical decelerating rf fields. In the magnicon, the output interaction is gyrotron–like, and requires a beam with substantial transverse momentum about the applied axial magnetic field. The transverse momentum is produced by spinning up the electron beam in a sequence of TM_{110} deflection cavities, the first driven by an external rf source. The output cavity employs an rf mode that rotates at the same frequency as the deflection cavity mode. As a result, the beam entering the output cavity is fully phase modulated with respect to the output cavity mode. The optimum magnetic field in the deflection cavities is approximately twice the cyclotron resonant value at the drive frequency. On the other hand, the output cavity operates as a first harmonic cyclotron device. These two constraints lead naturally to the design of a second–harmonic amplifier, in which the output cavity operates at twice the frequency of the deflection cavities and employs a TM_{210} mode (see Fig. 1). This is the configuration that is under investigation at NRL, as well as at the Budker Institute of Nuclear Physics (INP).

TWO CAVITY GAIN EXPERIMENTS

Figure 2 shows the results of a preliminary two–deflection–cavity gain experiment (5). This experiment was carried out using the NRL Long–Pulse Accelerator (LPA) Facility, and employed a field emission from a velvet cathode to produce a ~500 kV, 170 A beam at a magnetic field of 8 kG. Both the measured gain and the
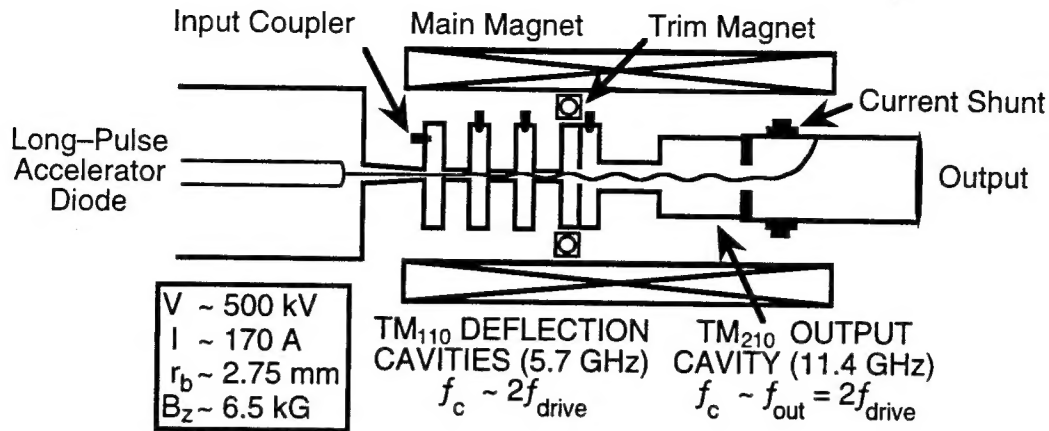
1

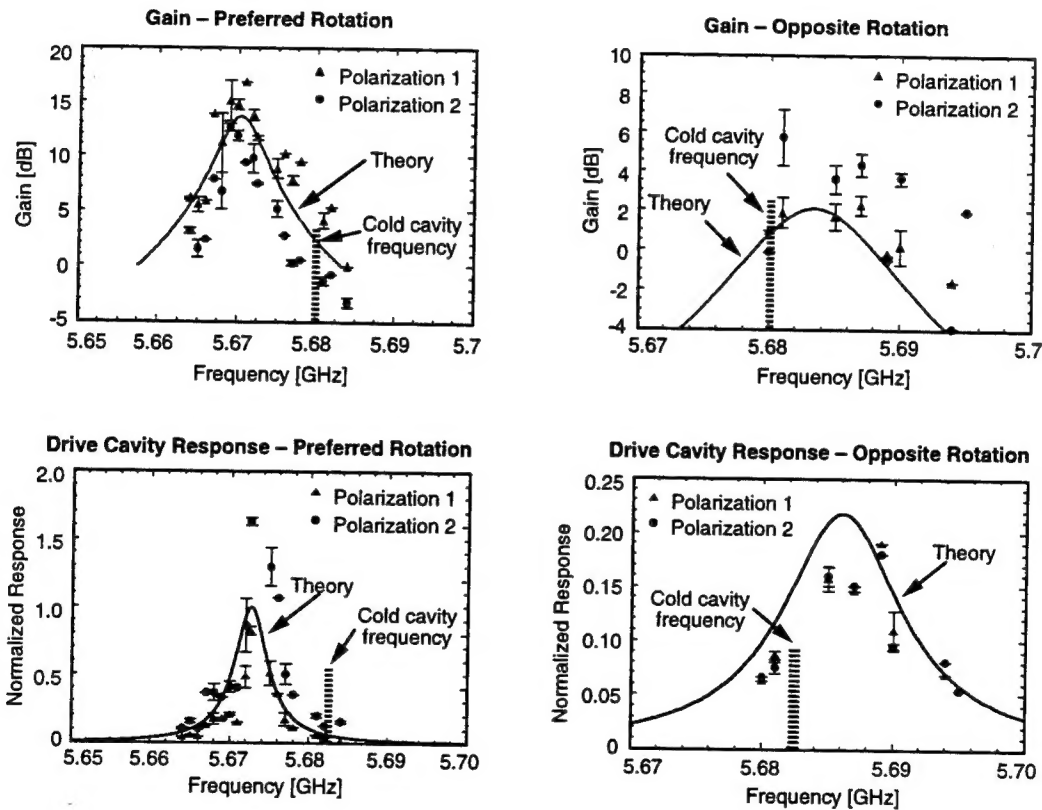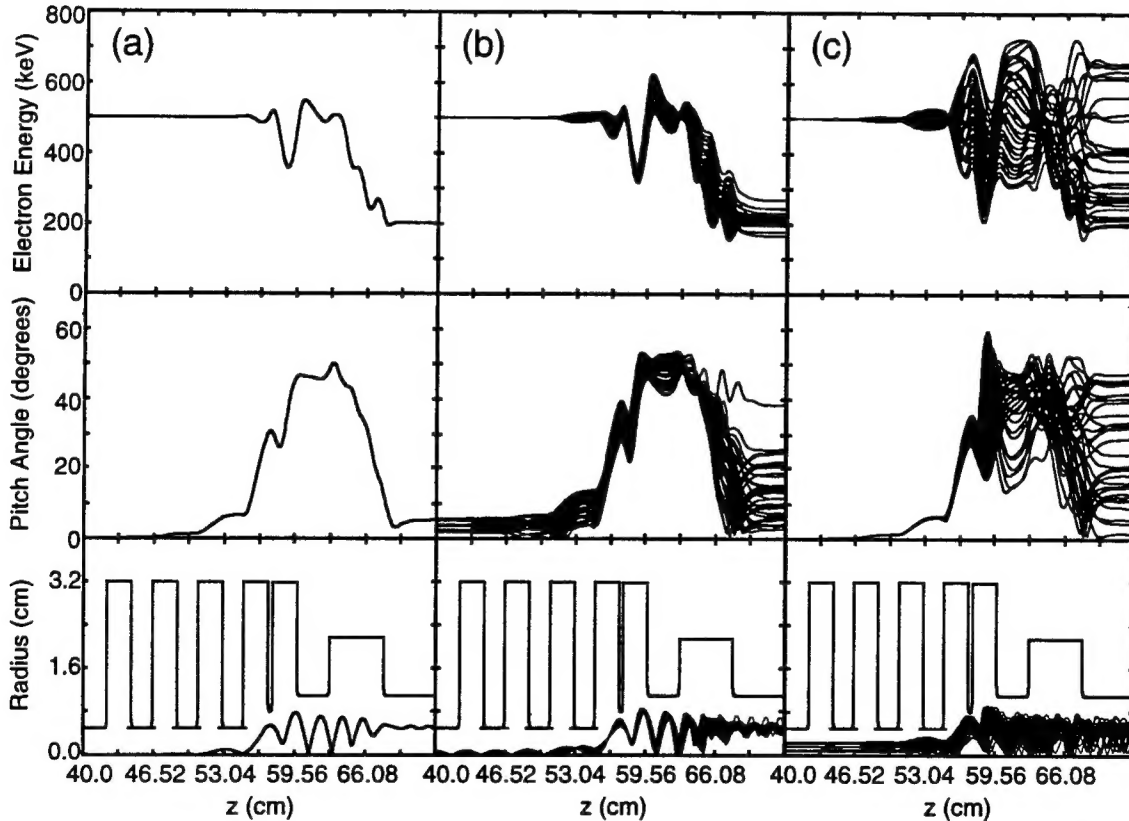**FIGURE 1.** Schematic diagram of the NRL magnicon amplifier

FIGURE 2. Results of the two–deflection–cavity gain experiment.

drive cavity response as a function of frequency agreed well with theory in both the preferred circular polarization, in which the electrons co–rotate with the rf mode, and in the opposite rotation. In the preferred rotation, a gain of ~15 dB was observed. However, it was also observed that the measured gain saturated at second–cavity signals equivalent to 1 to 10 kW of intracavity power. This very low field saturation effect was unexpected from linear magnicon theory, and was attributed to nonlinear loading of the cavity due to a multipactor–like process.

2

DESIGN OF AN 11.4 GHZ MAGNICON AMPLIFIER

A complete 11.4 GHz frequency–doubling magnicon amplifier circuit as illustrated in Fig. 1 was designed via computer simulation (6). Figure 3 shows the results of computer simulations of the operation of this circuit for a single electron, and for two finite electron beam diameters. These three simulations were all designed to have a pitch angle of approximately 45° at the end of the penultimate cavity, i.e., $\alpha = v_\perp / v_\parallel \sim 1$, where $v_\perp$ and $v_\parallel$ are the electron velocity components perpendicular and parallel to the applied magnetic field. Both the single particle and 2–mm–diam. simulations achieve efficiencies of ~56%. (The 2 mm beam diameter corresponds to the predicted performance of the INP thermionic magnicon electron gun (7) when matched into a 6.5 kG magnetic field.) However, the 5.5–mm–diam. simulation, corresponding to the present diameter of the NRL beam, achieves an efficiency of only ~23% due to the substantial energy spread and phase–mixing of the beam entering the output cavity. This result shows the necessity of using very small diameter electron beams to achieve efficient magnicon operation.

FIGURE 3. Steady–state magnicon simulations for a) a single electron, b) a 2–mm–diam. beam, and c) a 5.5–mm–diam. beam. The top traces show the electron energy, the middle traces show the electron pitch angles, and the bottom traces show the electron trajectories.

INITIAL TESTS OF THE MAGNICON CIRCUIT

The complete five cavity circuit, including a drive cavity, two gain cavities, and a penultimate cavity, all operating at ~5.7 GHz, followed by an output cavity designed to operate at ~11.4 GHz, was fabricated, cold tested, calibrated, and placed under vacuum on the LPA Facility. The cavities are fabricated from stainless steel, with a thin flash of copper to decrease the ohmic losses. They are held together with bolts, using viton O–rings to maintain the vacuum seals and copper gaskets to maintain the rf seals. The experiment is pumped from both the diode and output ends by cryopumps. Each of the cavities has a calibrated rf pickup, and the output from the last cavity can also be monitored at the end of the experiment using an X–band microwave horn. The various rf signals are measured using calibrated attenuators and crystal detectors. The first cavity is driven by rf from a tunable C–band magnetron.

Initial tests were carried out at the design voltage of 500 kV, the design current of ~170 A, and at magnetic fields ranging from 6.5–10 kG. The electron beam was again produced from a velvet cathode using field emission. The voltage pulse consists of a 100 nsec risetime, a ~300 nsec flattop, and a 500 nsec falltime. During the voltage falltime, the diode impedance collapses, often resulting in substantially larger currents than during the voltage flattop. In addition, the deflection cavity gain tends to increase as the voltage falls (8). As a result, oscillation often occurs during the trailing voltage pulse. However, the signal at the voltage flattop seems to correspond to stable amplification. The initial tests of the complete magnicon circuit demonstrated high gain (~40 dB) in the deflection cavities at low values of the drive signal, but showed a nonlinear saturation effect in the deflection cavities at higher drive signals, as previously seen in the two–deflection–cavity experiment. As the drive power was increased, on a shot–to–shot basis, the signal in each of the deflection cavities appeared to saturate in the range of 1–10 kW. In addition, small signals (<100 kW) were seen from the output cavity. Experiments then demonstrated that the saturation effect was related to the x–ray pulse from the diode, and was most likely due in addition to inadequate vacuum and surface conditions in the cavities. Specifically, the saturation effect appears to be due to plasma formation in the cavities, initiated by the x–ray pulse, and sustained by the microwaves. This plasma constitutes a nonlinear load on the cavities, which tends to clamp the microwave signal in the 1–10 kW power range, without completely shorting out the cavities. As a result, the predicted ~40 dB gain from the drive cavity to the penultimate cavity could only be observed experimentally with drive signals in the mW range.

A major effort was made to improve the vacuum conditions. One of the difficulties was the very limited vacuum conductance involved in pumping the deflection cavities through the beam pipe. This was improved by adding a pair of parallel pumping tubes that connect the first three deflection cavities to the main diode vacuum. In addition, the cavities were disassembled, thoroughly cleaned with detergents and solvents, and then reassembled and put through a low–temperature (~120° C) bakeout. Following this, a new set of measurements were begun. The low power saturation effect was still seen under the usual conditions of current and voltage. However, at higher currents and voltages (e.g., 650 kV and 300 A), a new regime of behavior was observed in the deflection cavities. These conditions should substantially increase the gain. What was observed during the voltage flattop were greatly increased signal levels from the second and third deflection cavities (with a nominal 1 kW signal in the first cavity), with the third cavity signal rising rapidly (~30 nsec) to approximately 1 MW, before apparently causing an rf breakdown of the third cavity. The penultimate cavity also reached high power (~100 kW) in a short pulse, before

4

collapsing. These signals correlate with the presence of a drive signal in the first cavity, and seem to correspond to stable amplification.

TIME–DEPENDENT SIMULATIONS OF THE OUTPUT CAVITY

The magnicon scanning–beam interaction creates a perfect synchronism between the beam position and the rf phase in the output cavity. That is, except for the slow–time–scale evolution of phase and amplitude in the output cavity prior to the achievement of steady–state conditions, the interaction is invariant in time. However, the beneficial effects of this perfect phase synchronism of the beam *as a whole* with the rf phase is degraded by any spreads in the beam parameters about the mean. Such spreads are produced in the process of spinning up the transverse beam momentum in the deflection cavities, as was seen in Fig. 3. A time–dependent simulation code was used to study the effects of various electron beam spreads on the interaction efficiency of the magnicon output cavity (9,10). These studies employed the realistic fields of the TM_{210} output cavity, including the effects of the entrance beam tunnel and the output iris. The baseline of these studies was the nominal parameters of the NRL magnicon design. Figure 4 shows typical results for the effects of α, γ, and gyroangle spread on the output efficiency.
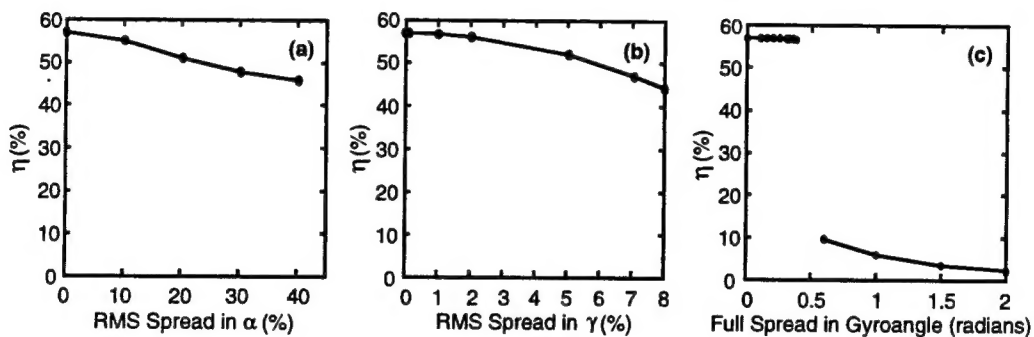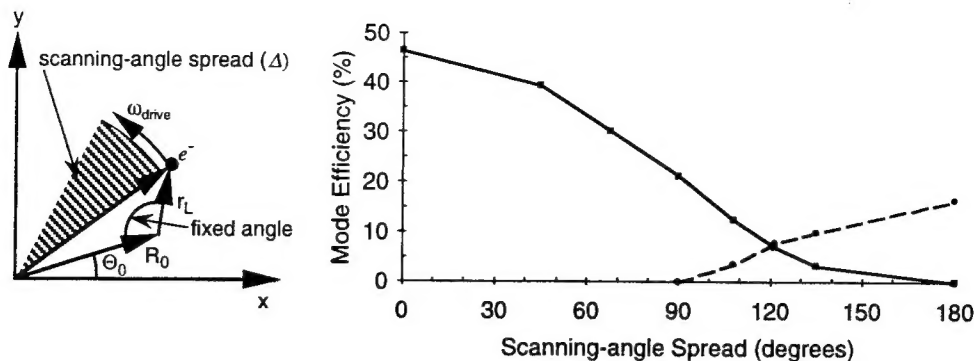

FIGURE 4. Effects of electron beam spreads on interaction efficiency.

An important problem in many gyrodevices is the competition between the various possible operating modes of the output cavity. The synchronous coupling between the beam and the rotating rf mode in the magnicon output cavity gives the magnicon interaction an important advantage compared to nonsynchronous gyrotron modes that may also couple to the transverse momentum of the electron beam. For a perfect beam, mode competition is not likely to be a problem. However, as the electron beam spreads increase, mode competition may become an issue. In a recent study (11), we used a time–dependent multimode code to examine the effect of one important spread, scanning–angle spread (see Fig. 5) on the competition between the synchronous TM_{210} magnicon mode and a nonsynchronous TE_{121} gyrotron mode of the output cavity. The TE_{121} mode appears to be the most dangerous competing mode because it lies close in frequency to the magnicon mode, and because it has substantial near–axis rf fields. Figure 5 shows a simulation of the final steady–state efficiency of the magnicon and gyrotron modes as a function of scanning angle spread. It is seen that up to spreads of ~90°, the magnicon interaction completely suppresses the gyrotron mode, while for greater spread angles, multimode states

FIGURE 5. Definition of scanning angle spread (left) and effect of scanning angle spread on magnicon efficiency and competition with TE_{121} gyrotron mode (right).

result. Finally, at 180°, which for an $m=2$ mode constitutes a complete loss of the beneficial effects of synchronism, the magnicon mode does not start, and what remains is a low efficiency gyrotron interaction.

FOURTH HARMONIC MAGNICON DESIGN

Both the NRL and INP magnicon experiments employ frequency doubling configurations, with the output cavity operating in the TM_{210} mode at the second harmonic of the drive frequency but in the first harmonic of the cyclotron frequency. This configuration has several significant advantages, since it leads to an approximately constant magnetic field throughout the magnicon circuit, and since it permits the deflection cavities to operate at half of the drive frequency, simplifying the task of spinning the electron beam up to high transverse momentum. It has been generally recognized that a synchronous magnicon interaction is possible in the mth harmonic of the drive frequency, provided that a mode with an azimuthal index of m is employed. However, since the magnicon beam produced by the deflection cavities is always near the cavity axis, the strength of the coupling generally decreases drastically for $m>2$, since the cavity modes become increasingly hollow. It has not been previously recognized that a fourth harmonic interaction, operating in the TM_{410} mode at the second harmonic of the cyclotron frequency, may also be feasible.

We are presently analyzing a fourth harmonic configuration at NRL (see Fig. 6). An important advantage is the lower frequency deflection system, which will lower rf fields, improve vacuum pumping, and perhaps relax the constraints on electron beam diameter. There are two reasons why this configuration is substantially more feasible than a first cyclotron harmonic frequency quadrupler. First, the electron beam, whose instantaneous guiding center is typically positioned slightly greater than one Larmor radius from the cavity axis, will be at twice the radius, since the required magnetic field is half as big. Second, because the strength of the coupling scales as $J_{m-s}(k_\perp r)$, where s is the cyclotron harmonic number and $k_\perp$ is the transverse wave number, a fourth harmonic, second cyclotron harmonic interaction will scale with radius as J_2 rather than J_3. Figure 7 compares the coupling for a second harmonic, first cyclotron harmonic interaction with fourth harmonic interactions operating in either the first or second cyclotron harmonic. This figure indicates that fourth harmonic, second cyclotron harmonic operation will require an approximate doubling of the rf electric field strength compared to second harmonic operation. However, the required fields, in the range of approximately 500 kV/cm, should be possible in a properly conditioned high vacuum output cavity.
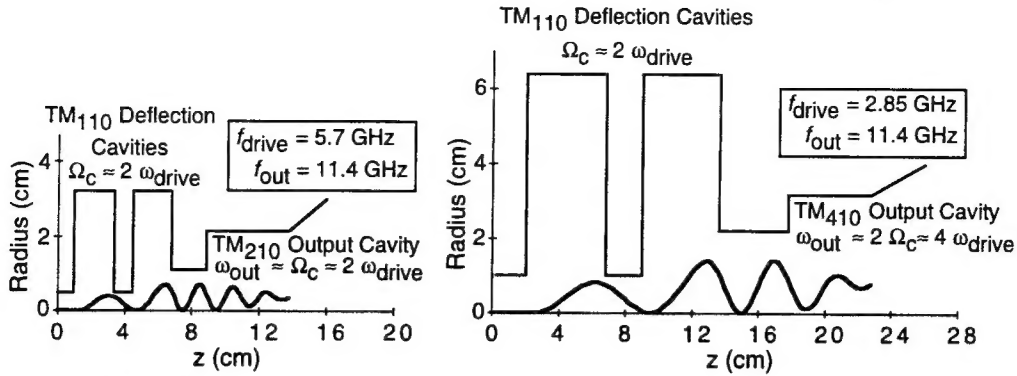
6

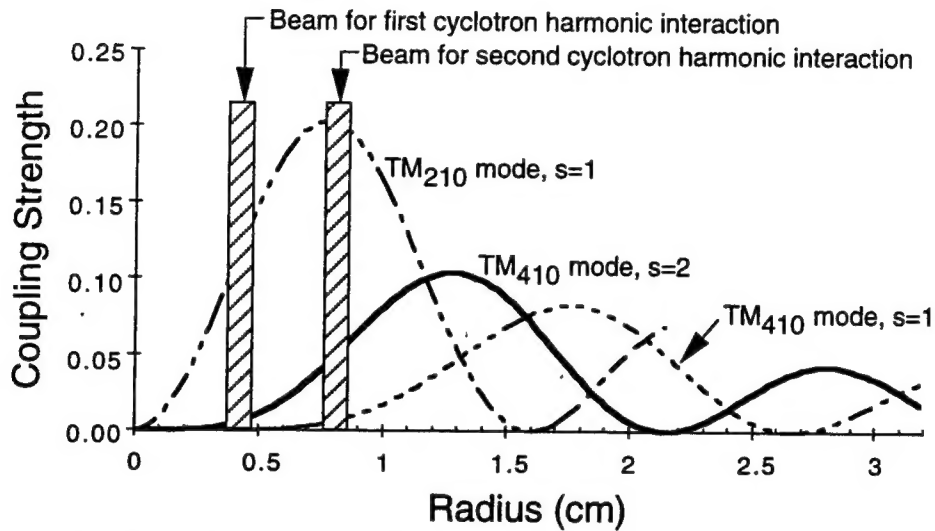**FIGURE 6.** Schematic of second and fourth harmonic magnicon designs.

FIGURE 7. Comparison of coupling for second and fourth harmonic magnicon designs.

CONCLUSIONS

The NRL magnicon experiment previously demonstrated the basic magnicon gain mechanism in two–deflection–cavity experiments. However, those experiments were forced to operate at very modest power levels to avoid an unanticipated gain saturation effect, that occurred as intracavity powers approached the kilowatt level. In the test of the full five cavity magnicon circuit, the same gain saturation effects were observed despite substantial improvements in the overall vacuum system. Experimental tests demonstrated that the saturation was due to plasma formation, caused by inadequate vacuum and surface conditions, and initiated by photoelectrons caused by the large x–ray flux from the accelerator diode region. A program of progressively improving the vacuum conditions, while at the same time pushing the envelope of magnicon parameters by operating at higher current, voltage, and magnetic field, has demonstrated that this low power saturation effect can be "burned through" in short (~30 nsec) high power pulses in the deflection cavities, often followed by rapid rf breakdown. However, this new regime of operation has not yet demonstrated high powers from the output cavity.

7

It is clear that the problems facing the present experiment are generic in nature, and are due to operation under vacuum conditions typical of pulsed power experiments rather than those typical of thermionic vacuum tubes. While high power, short pulse TE–mode gyrotrons have operated successfully under these conditions (12), it is apparent that magnicon cavities have more stringent requirements with respect to vacuum and surface conditions. The required field gradients in the present magnicon design are no greater than those in a comparable X–band klystron, and 50 MW X–band klystrons have been successfully operated with pulse lengths up to 1 μsec. However, the vacuum culture in those experiments, including high temperature brazes, all metal seals, extensive bakeout at very high temperatures (~500° C), and conditioning at high repetition rate, are impossible in an experiment designed to operate on a single–shot pulser using a plasma cathode. A practical magnicon amplifier will require all of the above. While it is still not clear what nature will permit for the single–shot NRL magnicon experiment, it is evident that this program must transition to a thermionic diode, a cw magnet, and a rep–rated modulator if substantial progress is to be made in demonstrating the feasibility of high power magnicon amplifiers at 11.4 GHz.

ACKNOWLEDGMENTS

REFERENCES

1. Karliner, M. M., Kozyrev, E. V., Makarov, I. G., Nezhevenko, O. A., Ostreiko, G. N., Persov, B. Z., and Serdobintsev, G. V., *Nucl. Instrum. Methods Phys. Res.* **A269**, 459–473 (1988).
2. Manheimer, W. M., *IEEE Trans. Plasma Sci* **18**, 632–645 (1990).
3. Nezhevenko, O. A., "The Magnicon: A New RF Power Source for Accelerators," in *Conf. Record—1991 IEEE Particle Accelerator Conf.*, edited by L. Lizama and J. Chew [IEEE, New York, 1991], vol. 5, pp. 2933–2942.
4. Nezhevenko, O. A., *IEEE Trans. Plasma Sci.*, October 1994, in press.
5. Gold, S. H., Sullivan, C. A., Hafizi, B., and Manheimer, W. M., *IEEE Trans. Plasma Sci.* **21**, 383–387 (1993).
6. Nezhevenko, O. A., Yakovlev, V. P., Gold, S. H., and Hafizi, B., *IEEE Trans. Plasma Sci.*, October 1994, in press.
7. Baryshev, B. A., Kazarezov, I. V., Kozyrev, E. V., Kuznetsov, G. I., Makarov, I. G., Nezhevenko, O. A., Persov, B. Z., Tiunov, M. A., Yakovlev, V. P., and Zapryagaev, I. A., *Nucl. Instrum. Methods Phys. Res.* **A340**, 241–258 (1994).
8. Hafizi, B., Seo, Y., Gold, S. H., Manheimer, W. M., and Sprangle, P. *IEEE Trans. Plasma Sci.* **20**, pp. 232–239, (1992).
9. Hafizi, B., Gold, S. H., Manheimer, W. M., and Sprangle, P., *Phys. Fluids B* **5**, 3045–3055 (1993).
10. Hafizi, B., and Gold, S. H., *Phys. Plasmas*, in press.
11. Fliflet, A. W., and Gold, S. H., submitted to *Phys. Plasmas*.
12. Black, W. M., Gold, S. H., Fliflet, A. W., Kirkpatrick, D. A., Manheimer, W. M., Lee, R. C., Granatstein, V. L., Hardesty, D. L., Kinkead, A. K., and Sucy, M., *Phys. Fluids B* **2**, 193–198 (1990).